Supporting Information

The XRD result shows that the film is mainly composed of LiV_3O_8 crystals with their [100] direction perpendicular to the substrate. Even though the film is uniform and close-packed, some scattered nanorods can be observed on the surface of the film as shown by the arrows in supplementary data Fig.S1. The nanorods are 150 nm long and 50 nm wide. The combination of the XRD results with supplementary data Fig.S1 demonstrate that the film is mainly composed of nanorods with (100) planes parallel to the substrate and (010) or (001) planes perpendicular to the substrate. The size of most crystals is about 50 nm wide and approximately 150 nm long.

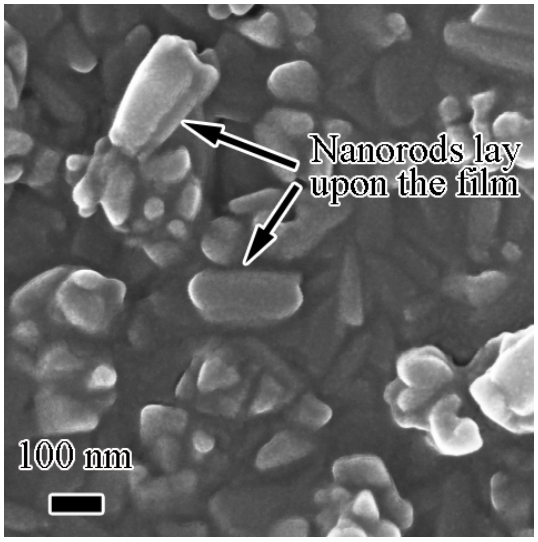

Figure S1 SEM image of the surface morphology of the nanostructured LiV_3O_8 thin film. Some random nanorods are indicated by the arrows

The further evidence for composition of amorphous wrapping is revealed by the TEM measurements. As we mentioned in the main text, the amorphous wrapping is metastable and a crystallization process occurs after continuous exposure to the electron beam. Fortunately, the transformation process can be clearly observed during the TEM measurement and the result is shown in supplementary data Fig.S2. Lattice fringes gradually appeared in the amorphous wrapping layer region and the spacing was measured to be 1.81 nm. This value agrees well with the spacing of (020) planes of the layered monoclinic LiV_3O_8. The TEM result indicates that the amorphous wrapping is composed of LiV_3O_8.

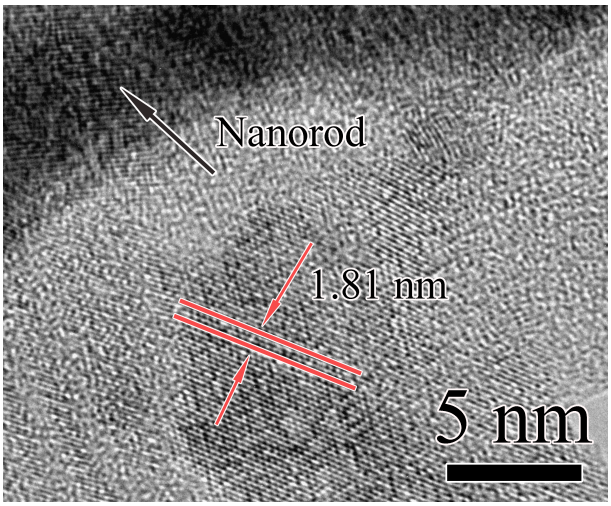

Figure S2 High-resolution TEM image of the amorphous wrapping after continuous exposure to the electron beam

Supplementary data figure S3 shows the XRD patterns of the LiV_3O_8 film deposited at different values of the sputtering oxygen partial pressure. There is no diffraction peak except for the substrate formed in a sputtering atmosphere of pure Ar, indicating that the main component of the film is amorphous. After increasing the ratio of Ar to O_2 in the gas mixture to 2:1, the crystalline component of the film is clearly LiV_3O_8 with no peaks associated with impurity phases. When altering the ratio of Ar/O_2 to 1:1, additional diffraction peaks are observed in the film and the $Li_{1.03}V_2O_5$ phase is observed. Overall, the crystallinity of the LiV_3O_8 film is enhanced with the increase of oxygen partial pressure. Supplementary data figure S4 shows the SEM image of the LiV_3O_8 thin film deposited with an Ar/O_2 ratio of 2:1. This shows particles 400 nm long with no heteropic compounds between them. The SEM image confirms that the crystallinity and particle size increase as a function of oxygen partial pressure.

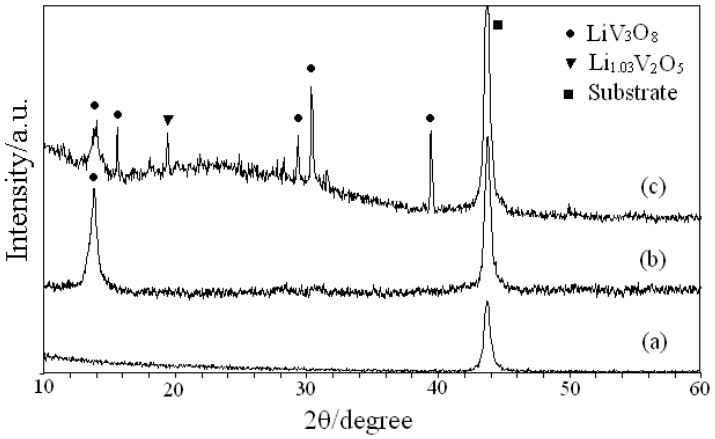

Figure S3 XRD pattern of as-deposited LiV_3O_8 thin film with different sputtering oxygen partial pressures (a) pure Ar, (b) $Ar:O_2$=2:1 and (c) $Ar:O_2$=1:1.

Figure S4 SEM image of LiV_3O_8 thin film prepared by RF sputtering at an Ar/O_2 ratio of 1:1.

Supplementary data figure S5 illustrates the evolution of the charge/discharge profile of LiV_3O_8 with its amorphous wrapped nanorods structure at both fast–charging and the normal-discharging rate. It is clear that even when the polarization becomes more pronounced when the charging rate increases to 20 C, the film still retains a high discharge capacity of 250 mAh g^{-1} at C/5. The rate performance is superior to all previous reports on LiV_3O_8 films.

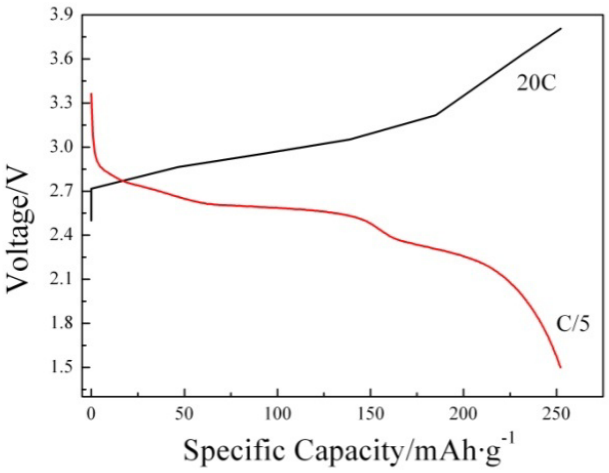

Figure S5 Charge/discharge curve for LiV_3O_8 with amorphous wrapped nanorod structure at fast–charging and normal-discharging rate.

An Arrhenius plot of $\ln(D_{Li+})$ as a function of $1/T$ is shown in supplementary data figure S6. According to solid state diffusion theory, the activation energy can be calculated from the well-known Arrhenius equation:

$$D_{Li+} = A\exp(-\frac{E_a}{RT}) \qquad (1)$$

where A is a temperature-independent coefficient, E_a is the activation energy, R is the gas constant (8.314 $J\cdot mol^{-1}\cdot K^{-1}$) and T is the absolute temperature. E_a is obtained from the slope of the linear fit of $\ln D_{Li+}$ against the reciprocal temperature, using the followed equation:

$$\ln D_{Li+} = a - \frac{E_a}{RT} \qquad (2)$$

According to equation 2, the activation energies of LiV_3O_8 with the amorphous wrapped nanorod structure at 2.8 V and 2.4 V are 73.3 and 65.7 kJ mol^{-1}, respectively, values which are lower than those of the mixed microstructure LiV_3O_8 electrode. The lower activation energies for LiV_3O_8 indicate the presence of shorter diffusion routes for Li ions intercalation.

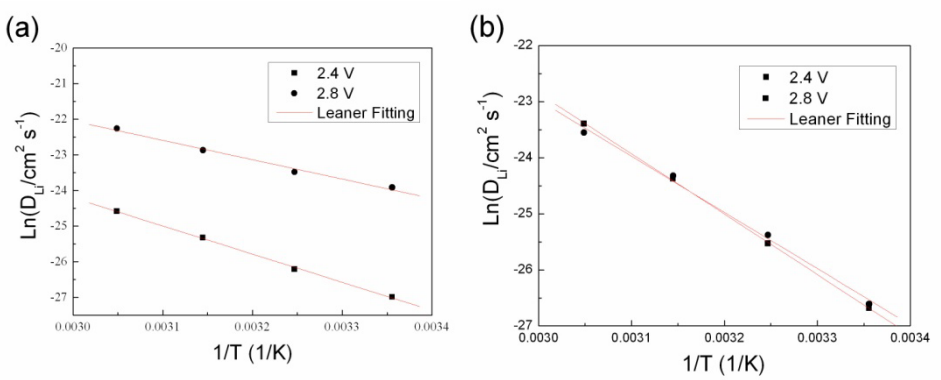

Figure S6 Arrhenius plots of $\ln(D_{Li+})$ versus 1/T for (a) amorphous wrapped nanorods and (b) mixed microstructure LiV_3O_8 thin film